



Deposited via The University of Sheffield.

White Rose Research Online URL for this paper:

<https://eprints.whiterose.ac.uk/id/eprint/133294/>

Version: Accepted Version

Proceedings Paper:

Dedeoglu, S. and Konstantopoulos, G. (2018) Three-phase grid-connected inverters equipped with nonlinear current-limiting control. In: Proceedings of 2018 UKACC 12th International Conference on Control (CONTROL). Control 2018: The 12th International UKACC Conference on Control, 05-07 Sep 2018, Sheffield, UK. IEEE, pp. 38-43. ISBN: 978-1-5386-2864-5.

<https://doi.org/10.1109/CONTROL.2018.8516764>

© 2018 IEEE. Personal use of this material is permitted. Permission from IEEE must be obtained for all other users, including reprinting/ republishing this material for advertising or promotional purposes, creating new collective works for resale or redistribution to servers or lists, or reuse of any copyrighted components of this work in other works. Reproduced in accordance with the publisher's self-archiving policy.

Reuse

Items deposited in White Rose Research Online are protected by copyright, with all rights reserved unless indicated otherwise. They may be downloaded and/or printed for private study, or other acts as permitted by national copyright laws. The publisher or other rights holders may allow further reproduction and re-use of the full text version. This is indicated by the licence information on the White Rose Research Online record for the item.

Takedown

If you consider content in White Rose Research Online to be in breach of UK law, please notify us by emailing eprints@whiterose.ac.uk including the URL of the record and the reason for the withdrawal request.

Three-Phase Grid-Connected Inverters Equipped with Nonlinear Current-Limiting Control

Seyfullah Dedeoglu and George C. Konstantopoulos
Department of Automatic Control and Systems Engineering
The University of Sheffield
Sheffield, S1 3JD, UK
{sdedeoglu1, g.konstantopoulos}@sheffield.ac.uk

Abstract—Voltage source inverters are essential devices to integrate renewable energy sources to the main grid and control the injection of real and reactive power. Due to their inherent nonlinear dynamics, the stability and particularly the current limitation of power controlled inverters represent challenging tasks under grid variations or unrealistic power demands. In this paper, using the synchronously rotating dq transformation, a nonlinear current limiting controller is proposed for three-phase inverters connected to the grid through an LCL filter. The proposed controller introduces a cascaded control structure with inner current and voltage control loops and an outer power controller that includes a droop function to support the grid and rigorously guarantee a limit for the grid currents. Using nonlinear closed-loop system analysis and based on input-to-state stability theory, the limits for the d- and q-axis grid currents are proven independently from each other without adding any saturation units into the system that can lead to instability. Extensive simulation results of the proposed nonlinear current-limiting controller are provided to demonstrate its effectiveness and current-limiting property.

Index Terms—Nonlinear control, three-phase inverter, current limitation, nonlinear stability analysis

I. INTRODUCTION

In contrast to traditional power grids which depend on the centralized generation, the smart grid architecture is based on several distributed generation (DG) units that include renewable energy sources, such as wind turbine generators and photovoltaic systems [1]. However, as the integration of the renewable sources into the grid increases, power system stability has become fragile due to volatility in the supply and demand which affects the frequency and voltage of the grid [2]. Therefore, in order to enhance system reliability and achieve large-scale utilization of DG units and seamless transition between islanded and grid-connected modes without violating the voltage and frequency limitations [3], the design of advanced control methods for the inverter devices that integrate DG systems to the main grid is of major importance [1], [4], [5]. Droop control is one of the most commonly used methods for inverters to support the grid, since it does not require any communication between the DG units and adjusts

the active and reactive power depending on the grid voltage and frequency [6].

Although droop control has been proven to be a very beneficial way to manage the injected active and reactive power independently, in a number of studies such as [7], [8], [9] and [10], the nonlinear dynamics of the controller and the system are often not taken into account and the stability analysis is based on linearization techniques. Since linearization methods confine the region of stability, the accurate nonlinear dynamics of a droop controlled grid-tied inverter should be considered for a rigorous stability analysis [11], [12].

In grid-connected applications, in order to improve the system stability and also protect the inverter and the filter against high currents, a current-limiting property should be additionally guaranteed. For this purpose, additional saturation blocks or limiters are often used in combination with the droop controller [13], [14], and [15]. However, these techniques can lead to instability due to integrator windup. This problem can be alleviated using anti-windup methods [16], [17], but most of the modern anti-windup methods need full information of the system parameters, which are generally unknown, and traditional anti-windup techniques cannot rigorously guarantee closed-loop system stability. To this end, a nonlinear current limiting controller that overcomes these issues has been recently proposed for single phase grid-connected inverters in [18], [19] and guarantees current limitation without suffering from integrator windup under both normal and faulty grid conditions. However, this controller cannot be directly applied to three-phase inverters using the dq synchronously rotating reference frame modelling [1] and can only limit the current on the inverter side and not the grid side, which is more important in grid-connected applications.

In this paper, a nonlinear controller that can be applied to three-phase inverters connected to the grid with an LCL filter and guarantee a rigorous grid current limitation is proposed. Based on the synchronously rotating dq reference frame modelling of the inverter, the proposed controller is designed in a cascaded control structure with two inner current and voltage loops and an outer power control loop (droop control). For the inner control loops, traditional PI controllers are adopted with decoupling terms to guarantee fast regulation of the inverter currents and voltage, which is a common approach

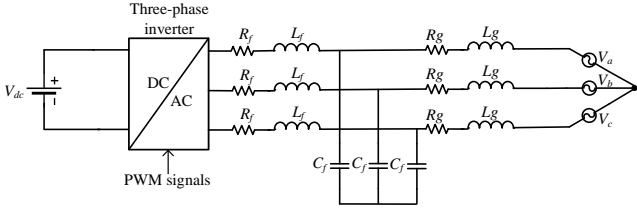


Fig. 1: Three-phase grid-connected inverter with an LCL filter

in three-phase inverter applications [20]. However, for the outer power loop, a new nonlinear droop controller is proposed with bounded voltage dynamics and a constant virtual resistance to guarantee closed-loop system stability and the desired limitation. Using nonlinear Lyapunov methods [21], the boundedness of the controller voltages are analytically proven and then using input-to-state stability, the d- and q-axis grid currents are proven to be limited below a given maximum value independently from each other or the power demand. Hence, the proposed controller introduces a droop control structure to support the voltage and frequency of the grid and at the same time maintains a limited injected current to the grid to protect the inverter under unrealistic power demands. Detailed simulation results of a grid-connected three-phase inverter equipped with the proposed nonlinear current-limiting controller are presented to verify the theoretical analysis.

The rest of the paper is arranged as follows. In Section II, the dynamic model of a three-phase grid-connected inverter is given. In Section III, the proposed controller is presented and the dynamics of the outer power control loop are analyzed to prove the desired current-limiting property. In Section IV, simulation results of a three-phase inverter operating under the proposed controller are provided and in Section V, the conclusions of the paper are drawn.

II. DYNAMIC MODEL OF THE SYSTEM

The system under consideration is a three-phase inverter connected to a balanced grid with angular velocity ω_g via an LCL filter, as illustrated in Fig. 1. The inverter-side filter resistance, inductance, and capacitance are represented by R_f , L_f , and C_f , respectively, while grid-side filter resistance and inductance are denoted as R_g and L_g . The inverter is supplied by a dc source denoted as V_{dc} , while V_a , V_b , and V_c represent the three-phase grid voltages. The dynamic model of the system can be obtained using the synchronously rotating dq frame [1], as given below:

$$L_f \frac{dI_{fd}}{dt} = -R_f I_{fd} + \omega L_f I_{fq} + m_d \frac{V_{dc}}{2} - V_{Cd} \quad (1)$$

$$L_f \frac{dI_{fq}}{dt} = -R_f I_{fq} - \omega L_f I_{fd} + m_q \frac{V_{dc}}{2} - V_{Cq} \quad (2)$$

$$C_f \frac{dV_{Cd}}{dt} = I_{fd} - I_{gd} + \omega C_f V_{Cq} \quad (3)$$

$$C_f \frac{dV_{Cq}}{dt} = I_{fq} - I_{gq} - \omega C_f V_{Cd} \quad (4)$$

$$L_g \frac{dI_{gd}}{dt} = -R_g I_{gd} + \omega L_g I_{gq} - V_{gd} + V_{Cd} \quad (5)$$

$$L_g \frac{dI_{gq}}{dt} = -R_g I_{gq} - \omega L_g I_{gd} - V_{gq} + V_{Cq} \quad (6)$$

where I_{fd} , I_{fq} and I_{gd} , I_{gq} represent the d and q components of inverter and grid currents, respectively, whereas V_{Cd} , V_{Cq} and V_{gd} , V_{gq} symbolize the filter and grid voltages in dq frame. The control inputs of the system are represented by m_d and m_q , which are duty ratio functions that drive the PWM (pulse width modulation) signals for the inverter. Taking into consideration the dq system equivalence, as in [22], the real power P and reactive power Q of the system can be calculated as

$$P = \frac{3}{2} (V_{Cd} I_{gd} + V_{Cq} I_{gq}), Q = \frac{3}{2} (V_{Cd} I_{gq} - V_{Cq} I_{gd}). \quad (7)$$

As can be seen from (7), due to the multiplication of the system states in the expressions of P and Q , any controller that requires the calculation of the real and the reactive power, such as the droop controller, will result in a nonlinear closed loop system. Hence, the stability analysis of the closed-loop system and key properties for the inverter, such as current limitation, must be proven using nonlinear systems theory. To this end, the main aim of this paper is to design a nonlinear droop controller for a three-phase inverter that guarantees stability and limits the grid currents under given maximum values at all times.

III. CONTROLLER DESIGN AND ANALYSIS

In order to design the desired droop controller for the inverter, a cascaded control structure which includes inner current and voltage control loops and an outer power control loop is adopted. For the inverter side currents and voltages, the inner loops introduce a PI controller with decoupling terms, while a novel nonlinear droop controller is proposed as the outer loop to limit the grid currents in dq reference frame as presented below in detail.

A. Inner Control Loops

Based on the dq dynamic model of the grid-connected inverter, where m_d and m_q are the control inputs, the inner current controller that regulates the inverter currents I_{fd} and I_{fq} to the desired values I_{dref} and I_{qref} , respectively takes the form:

$$m_d = \frac{(I_{dref} - I_{fd})(K_{pi} + \frac{K_{I_i}}{s}) + V_{Cd} - \omega L_f I_{fq}}{0.5V_{dc}} \quad (8)$$

$$m_q = \frac{(I_{qref} - I_{fq})(K_{pi} + \frac{K_{I_i}}{s}) + V_{Cq} + \omega L_f I_{fd}}{0.5V_{dc}}.$$

Here, a PI controller with additional decoupling terms is applied at the duty-ratio inputs m_d and m_q , while the reference values I_{dref} and I_{qref} are obtained from a voltage controller with similar structure:

$$I_{dref} = (V_{Cdref} - V_{Cd})(K_{pv} + \frac{K_{I_v}}{s}) + I_{gd} - \omega C_f V_{Cq} \quad (9)$$

$$I_{qref} = (V_{Cqref} - V_{Cq})(K_{pv} + \frac{K_{I_v}}{s}) + I_{gq} + \omega C_f V_{Cd}$$

where the desired values for the capacitor voltages V_{Cdref} and V_{Cqref} are defined by the outer power control loop.

The PI controller gains can be selected accordingly such that the current controller acts much faster than the voltage controller, which acts faster than the power controller. This design of controllers in different time scales can be accomplished via suitable pole placement and is widely adopted in a cascaded control design approach [23].

B. Proposed Nonlinear Controller (Outer Loop)

Since the fast inner control loops have been extensively investigated in the literature [13] and [23], this paper will focus on the design of the outer droop control loop, which represents the novelty of this work. Based on the fast current and voltage controllers, it is considered that the capacitor voltages V_{Cd} and V_{Cq} are regulated to their reference values V_{Cdref} and V_{Cqref} in (5) and (6). Then, the proposed controller takes the form

$$V_{Cdref} = V_{gd} + E_d - r_v I_{gd} - \omega L_g I_{gq} \quad (10)$$

$$V_{Cqref} = V_{gq} + E_q - r_v I_{gq} + \omega L_g I_{gd} \quad (11)$$

In (10) and (11), the parameters E_d and E_q represent two controllable voltage terms (controller states) that implement the desired droop functions, while r_v acts as a positive constant virtual resistance. Inspired by the universal droop control expressions [24], and the bounded controller designed in [25], the controller states E_d and E_q are dynamically formed as

$$\dot{E}_d = c_d (K_e(E^* - V_C) - n(P - P_{set})) E_{dq}^2 \quad (12)$$

$$\begin{aligned} \dot{E}_{dq} = & -\frac{c_d E_d E_{dq}}{E_{max}^2} (K_e(E^* - V_C) - n(P - P_{set})) \\ & - k_d \left(\frac{E_d^2}{E_{max}^2} + E_{dq}^2 - 1 \right) E_{dq} \end{aligned} \quad (13)$$

$$\dot{E}_q = -c_q (\omega^* - \omega_g + m(Q - Q_{set})) E_{qq}^2 \quad (14)$$

$$\begin{aligned} \dot{E}_{qq} = & \frac{c_q E_q E_{qq}}{E_{max}^2} (\omega^* - \omega_g + m(Q - Q_{set})) \\ & - k_q \left(\frac{E_q^2}{E_{max}^2} + E_{qq}^2 - 1 \right) E_{qq} \end{aligned} \quad (15)$$

where E_{dq} , and E_{qq} are two additional control states and c_d , c_q , E_{max} , K_e , k_d , and k_q are positive constants. The expression $K_e(E^* - V_C) - n(P - P_{set})$ introduces the $P \sim V$ droop expression, which should be zero at the steady-state, and E^* is the rated RMS voltage of the grid, V_C is the RMS voltage of the filter capacitor given as $V_C = \sqrt{\frac{V_{Cd}^2 + V_{Cq}^2}{2}}$, P_{set} is the reference value of the real power and n is the droop coefficient. Similarly, $\omega^* - \omega_g + m(Q - Q_{set})$ represents the $Q \sim -\omega$ droop expression, where ω^* is the rated angular frequency, ω_g is the grid frequency, Q_{set} is the desired injected reactive power and m is the second droop coefficient. The $P \sim V$ and $Q \sim -\omega$ droop expressions are adopted in this paper due to the introduction of the virtual resistance r_v in the output via the proposed control design [24]. The initial conditions of the controller states E_d , E_{dq} , E_q , and E_{qq} are selected as 0, 1, 0, and 1, respectively, and the nonlinear dynamics (12)-(15) have been proposed in a way to guarantee the boundedness of the controller states E_d and E_q in the

range $E_d, E_q \in [-E_{max}, E_{max}]$ as explained below.

For the controller dynamics (12) and (13), one can consider a Lyapunov function candidate as

$$W_d = \frac{E_d^2}{E_{max}^2} + E_{dq}^2. \quad (16)$$

The time derivative of this function is

$$\dot{W}_d = \frac{2E_d \dot{E}_d}{E_{max}^2} + 2E_{dq} \dot{E}_{dq}. \quad (17)$$

By replacing in (17) \dot{E}_d and \dot{E}_{dq} from the controller dynamics (12) and (13), then

$$\dot{W}_d = -2k_d \left(\frac{E_d^2}{E_{max}^2} + E_{dq}^2 - 1 \right) E_{dq}^2. \quad (18)$$

As can be seen from (18), $\dot{W}_d = 0$ when $E_{dq} = 0$ or for every values of E_d and E_{dq} on the ellipse:

$$W_{d0} = \left\{ E_d, E_{dq} \in R : \frac{E_d^2}{E_{max}^2} + E_{dq}^2 = 1 \right\}. \quad (19)$$

Based on the initial conditions of the controller states, E_d and E_{dq} will always stay on the ellipse W_{d0} as mathematically expressed below:

$$\dot{W}_d = 0 \Rightarrow W_d(t) = W_d(0) = 1, \quad \forall t \geq 0. \quad (20)$$

Hence, $E_d \in [-E_{max}, E_{max}]$, $\forall t \geq 0$. By considering the transformation

$$E_d = E_{max} \sin \phi \quad \text{and} \quad E_{dq} = \cos \phi \quad (21)$$

then taking into account (12)-(13), E_d and E_{dq} will travel on the ellipse W_{d0} with an angular velocity

$$\dot{\phi} = \frac{c_d (K_e(E^* - V_C) - n(P - P_{set})) E_{dq}}{E_{max}}. \quad (22)$$

From (22), when $K_e(E^* - V_C) - n(P - P_{set})$ is zero, the angular velocity becomes zero and the controller states can converge to the desired equilibrium point defined by the $P \sim V$ droop control. Considering a similar analysis for the controller dynamics (14)-(15), then E_q and E_{qq} are proven to remain on a similar ellipse

$$B_{q0} = \left\{ E_q, E_{qq} \in R : \frac{E_q^2}{E_{max}^2} + E_{qq}^2 = 1 \right\} \quad (23)$$

and travel with angular velocity

$$\dot{\psi} = \frac{-c_q (\omega^* - \omega_g + m(Q - Q_{set})) E_{qq}}{E_{max}}. \quad (24)$$

Therefore, the $Q \sim -\omega$ droop can be implemented in a similar way, while E_q satisfies $E_q \in [-E_{max}, E_{max}] \forall t \geq 0$.

It should be noted that, the proposed controller can easily change from the droop control to accurate regulation of P and Q at their reference values by removing the term $K_e(E^* - V_C)$ from (12)-(13) and the term $\omega^* - \omega_g$ from (14)-(15). Thus, real and reactive power can be set to their desired values at any time and transition between the two modes can be seamlessly

realized.

C. Stability analysis and current-limiting property

By implementing the proposed controller (10)-(11) into the grid side current equations (5)-(6) and taking into account the fast regulation of the inner current and voltage loops, the closed-loop grid-side current equations are expressed as

$$L_g \frac{dI_{gd}}{dt} = -(R_g + r_v)I_{gd} + E_d \quad (25)$$

$$L_g \frac{dI_{gq}}{dt} = -(R_g + r_v)I_{gq} + E_q \quad (26)$$

It is clear that the dynamics of I_{gd} and I_{gq} can be handled independently taking into account that $E_d, E_q \in [-E_{max}, E_{max}]$ for all $t \geq 0$, as proven in the previous subsection. Hence for d -axis grid current dynamics (26), consider the Lyapunov function candidate as

$$V = \frac{1}{2}L_g I_{gd}^2. \quad (27)$$

The time derivative of V is calculated using (25) as

$$\begin{aligned} \dot{V} &= -(R_g + r_v)I_{gd}^2 + E_d I_{gd} \\ &\leq -(R_g + r_v)I_{gd}^2 + |E_d||I_{gd}|. \end{aligned} \quad (28)$$

Thus,

$$\dot{V} < 0, \forall |I_{gd}| > \frac{|E_d|}{R_g + r_v} \quad (29)$$

which proves that system (25) is input-to-state stable by considering E_d as the input. Since it is proven that $|E_d| \leq E_{max}$, $\forall t \geq 0$, then I_{gd} will be bounded for all $t \geq 0$. In particular, if initially $|I_{gd}(0)| \leq \frac{E_{max}}{R_g + r_v}$ then from the input-to-state stability analysis, there is

$$|I_{gd}(t)| \leq \frac{E_{max}}{R_g + r_v}, \forall t \geq 0. \quad (30)$$

In order to limit the current I_{gd} below a maximum value I_{max} , the controller parameters E_{max} and r_v can be suitably selected to satisfy

$$E_{max} = (R_g + r_v)I_{max}. \quad (31)$$

By substituting (31) into (30), it is proven that

$$|I_{gd}(t)| \leq I_{max}, \forall t \geq 0, \quad (32)$$

which proves the desired current-limiting property.

A similar approach for the q -axis grid current dynamics (26) can easily show that if initially it holds that $|I_{gq}(0)| \leq \frac{E_{max}}{R_g + r_v}$, then

$$|I_{gq}(t)| \leq I_{max}, \forall t \geq 0. \quad (33)$$

As a result, the grid currents are proven to remain below a defined maximum value I_{max} independently from each order or the nonlinear droop control expressions by suitably selecting the controller parameters E_{max} and r_v according to (31). This is achieved without using any saturation units, which is a common approach in conventional controllers and can lead to instability [13]-[14]. Since the current-limiting

property is achieved using nonlinear Lyapunov theory and input-to-state stability analysis, then the grid current limitation is guaranteed at all times, even during transients. It is worth mentioning that if $|I_{gd}| \rightarrow I_{max}$ or $|I_{gq}| \rightarrow I_{max}$, then $|E_d| \rightarrow E_{max}$ or $|E_q| \rightarrow E_{max}$, respectively, which leads to $E_{dq} \rightarrow 0$ or $E_{qq} \rightarrow 0$ since the controller states are restricted on the ellipses W_{d0} and B_{q0} . Then from (12) and (14), it becomes clear that $\dot{E}_d \rightarrow 0$ and $\dot{E}_q \rightarrow 0$, which proves that the integration slows down near the limits resulting in an inherent anti-windup property of the proposed controller. This highlights the superiority of the proposed controller with respect to existing approaches that introduce saturation limits and require additional anti-windup mechanisms that further complicate the controller implementation and closed-loop system stability analysis.

TABLE I: System and controller parameters

Parameters	Values	Parameters	Values
L_f, L_g	0.0139H	C_f	1.8186 μ F
R_f, R_g	0.8752 Ω	r_v	2 Ω
n	0.0661	m	0.0019
ω_g	2 π 49.97 rad/s	k_d, k_q	1
V_{dc}	700V	I_{max}	2.5A
K_e	10	K_{Pv}, K_{Iv}	2, 10
K_{Pi}, K_{Ii}	0.3, 10	ω^*	2 π 50 rad/s
c_d	0.65	E^*	218V
c_q	22.5	E_{max}	7.188V
V_{gd}	220 $\sqrt{2}$ V	V_{gq}	0V

IV. SIMULATION RESULTS

In order to validate the effectiveness of the proposed control strategy, a three-phase grid-connected inverter is simulated using the Matlab/Simulink software. The system and controller parameters are given in Table I. In this section, the main aim is to illustrate that the proposed controller can change between set mode, i.e. accurate real and reactive power regulation and droop control mode and at the same time limits the grid currents when an unrealistic power reference value is provided to the controller.

Initially, the set control mode is enabled by removing the terms $K_e(E^* - V_C)$ and $\omega^* - \omega_g$ from (12)-(13) and (14)-(15), respectively, where P_{set} and Q_{set} are set to zero. At the time instant $t = 1s$, the active power reference value P_{set} changes to 400 W and at $t = 2s$, it is further increased to 1650 W. As it can be seen from Fig. 2, initially P is regulated to the desired 400W value but when P_{set} becomes very high, the proposed controller regulates the real power to a lower value. This is because the current I_{gd} tries to violate its maximum value $I_{max} = 2.5A$ in Fig. 4 and the proposed controller maintains the desired current limitation to protect the inverter under unrealistic power demands. However, the reactive power is always regulated to the desired zero value and the current I_{gq} remains also limited below its maximum value. At $t = 3s$,

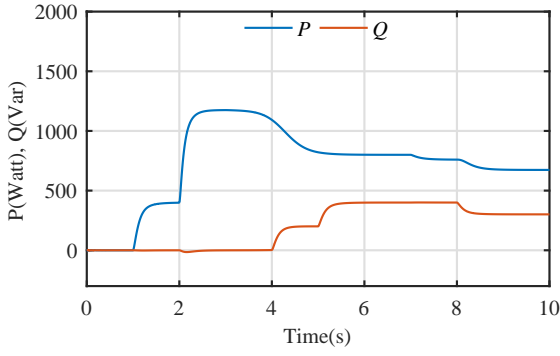


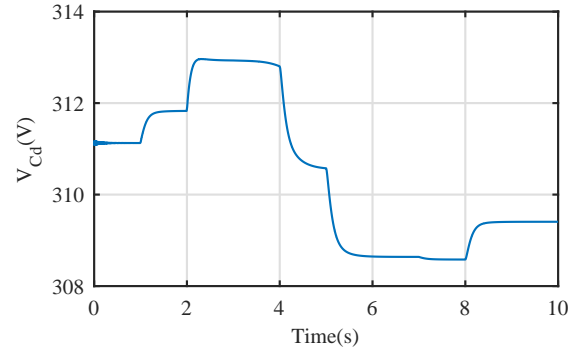
Fig. 2: Real and reactive power

P_{set} is decreased to 800 W and the real power is regulated to the desired value after a short transient. At the time instant $t = 4s$, the reactive power reference Q_{set} increases to 200 Var and at $t = 5$ it changes to 400 Var to verify the ability of the controller to regulate the reactive power. As it can be seen from Fig. 2, the reactive power injected by the inverter is accurately regulated to both reference values. The $P \sim V$ droop control is enabled at $t = 7s$, and the real power decreases to 760 W in order to regulate the RMS voltage V_C closer to the rated E^* . The response of the system states V_{Cd} and V_{Cq} , which define the RMS value V_C as $V_C = \sqrt{\frac{V_{Cd}^2 + V_{Cq}^2}{2}}$, is shown in Fig. 3. At the time instant $t = 8s$, the $Q \sim -\omega$ droop control is enabled and the reactive power is decreased to 301 Var since the frequency of the grid ω_g is slightly lower than the rated ω^* , as given in the parameters of Table I. Hence, both accurate regulation of the real and reactive power and droop control modes can be implemented by the proposed nonlinear controller with an inherent grid current limitation that protects the inverter from unrealistic values of the power demand.

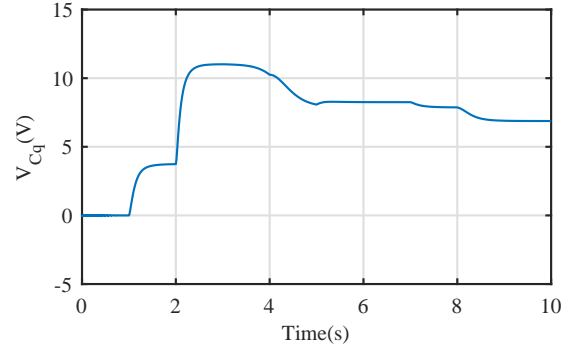
In order to verify the theoretic analysis, the trajectory of the controller states E_d, E_{dq} and E_q, E_{qq} is plotted on the $E_d - E_{dq}$ and $E_q - E_{qq}$ planes, respectively, in Fig. 5 for the entire simulation. One can easily observe that the controller states remain on the corresponding ellipses W_{d0} and B_{q0} , which are the same in this case. From the controller analysis, as the state E_{dq} tends to zero, state E_d reaches its maximum value E_{max} , as shown in Fig. 5, leading to the current-limiting property for I_{gd} . Since I_{gq} does not reach its upper limit (Fig. 4), then the trajectory of the controller states E_q and E_{qq} remains on the top of the ellipse B_{q0} and is regulated at the corresponding steady-state values depending on the reference value Q_{set} and the $Q \sim -\omega$ droop.

V. CONCLUSIONS

A nonlinear current-limiting droop controller for a three-phase inverter connected to the grid through and LCL filter was proposed in this paper. The proposed controller includes traditional PI controllers with decoupling terms for the inner control loops and a nonlinear dynamic controller for the outer



(a) d-axis capacitor voltage



(b) q-axis capacitor voltage

Fig. 3: Filter capacitor voltages

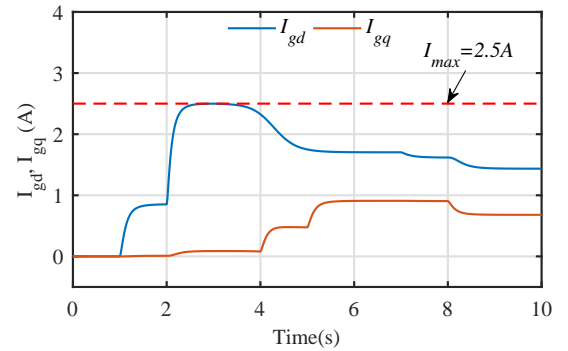


Fig. 4: d- and q-axis grid currents

power control loop. Using the nonlinear dynamics of the system and input-to-state stability theory, the current-limiting property of the grid-side inverter currents was analytically proven based on the bounded controller dynamics and the virtual resistance that was introduced in the proposed control design. Both active and reactive power regulation and droop control with a guaranteed upper limit for the grid currents can be accomplished by the proposed nonlinear controller, which was validated via extensive simulation results of a grid-connected three-phase inverter to support the theoretical analysis of the proposed control approach.

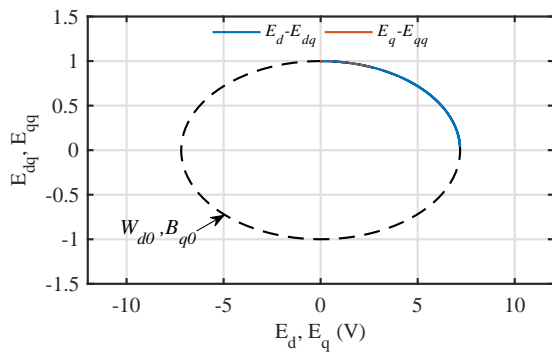


Fig. 5: Controller states E_d, E_{dq} and E_q, E_{qq}

REFERENCES

- [1] Q.-C. Zhong, T. Hornik, *Control of Power Inverters in Renewable Energy and Smart Grid Integration*, New York, NY, USA: Wiley-IEEE Press, 2013.
- [2] J. M. Carrasco *et al.*, "Power-Electronic Systems for the Grid Integration of Renewable Energy Sources : A Survey," *IEEE Trans. Ind. Electron.*, vol. 53, no. 4, pp. 1002–1016, 2006.
- [3] "The grid code," *National Grid Electricity Transmission PLC*, London, U.K., Tech. Rep., Dec. 2010.
- [4] Q.-C. Zhong, G. Weiss, "Synchronverters: Inverters that mimic synchronous generators," *IEEE Trans. Ind. Electron.*, vol. 58, no. 4, pp. 1259–1267, Apr. 2011.
- [5] J. M. Guerrero, J. Matas, L. G. de Vicuna, M. Castilla, J. Miret, "Decentralized control for parallel operation of distributed generation inverters using resistive output impedance," *IEEE Trans. Ind. Electron.*, vol. 54, no. 2, pp. 994–1004, Nov. 2007.
- [6] Y. Han, H. Li, P. Shen, E. A. A. Coelho, and J. M. Guerrero, "Review of Active and Reactive Power Sharing Strategies in Hierarchical Controlled Microgrids," *IEEE Trans. Power Electron.*, vol. 32, no. 3, pp. 2427–2451, 2017.
- [7] R. Majumder, "Some aspects of stability in microgrids," *IEEE Trans. Power Syst.*, vol. 28, no. 3, pp. 3243–3252, Aug. 2013.
- [8] X. Tang, W. Deng, Z. Qi, "Investigation of the dynamic stability of microgrid," *IEEE Trans. Power Syst.*, vol. 29, no. 2, pp. 698–706, Mar. 2014.
- [9] R. Majumder, B. Chaudhuri, A. Ghosh, G. Ledwich, F. Zare, "Improvement of stability and load sharing in an autonomous microgrid using supplementary droop control loop," *IEEE Trans. Power Syst.*, vol. 25, no. 2, pp. 796–808, May 2010.
- [10] Y. Mohamed, E. El-Saadany, "Adaptive decentralized droop controller to preserve power sharing stability of paralleled inverters in distributed generation microgrids," *IEEE Trans. Power Electron.*, vol. 23, no. 6, pp. 2806–2816, Nov. 2008.
- [11] J. Schiffer, D. Zonetti, R. Ortega, A. Stankovic, T. Sezi, J. Raisch, "A survey on modeling of microgrids—From fundamental physics to phasors and voltage sources," *Automatica*, vol. 74, pp. 135–150, 2016.
- [12] E. Lenz Cesar, D. J. Pagano, and J. Pou, "Bifurcation Analysis of Parallel-Connected Voltage-Source Inverters with Constant Power Loads," *IEEE Trans. Smart Grid*, vol. 3053, no. c, pp. 1–1, 2017.
- [13] H. Xin, L. Huang, L. Zhang, Z. Wang, J. Hu, "Synchronous instability mechanism of P-f droop-controlled voltage source converter caused by current saturation," *IEEE Trans. Power Syst.*, vol. 31, no. 6, pp. 5206–5207, Nov. 2016.
- [14] N. Bottrell, T. C. Green, "Comparison of current-limiting strategies during fault ride-through of inverters to prevent latch-up and wind-up," *IEEE Trans. Power Electron.*, vol. 29, no. 7, pp. 3786–3797, Jul. 2014.
- [15] A. D. Paquette, D. M. Divan, "Virtual impedance current limiting for inverters in microgrids with synchronous generators," *IEEE Trans. Ind. Appl.*, vol. 51, no. 2, pp. 1630–1638, Mar./Apr. 2015.
- [16] L. Zaccarian, A. R. Teel, "Nonlinear scheduled anti-windup design for linear systems," *IEEE Trans. Autom. Control*, vol. 49, no. 11, pp. 2055–2061, Nov. 2004.
- [17] S. Tarbouriech, M. Turner, "Anti-windup design: An overview of some recent advances and open problems," *IET Control Theory Appl.*, vol. 3, no. 1, pp. 1–19, Jan. 2009.
- [18] Q.-C. Zhong and G. C. Konstantopoulos, "Current-Limiting Droop Control of Grid-connected Inverters," *IEEE Trans. Ind. Electron.*, vol. 46, no. c, pp. 1–1, 2016.
- [19] G. C. Konstantopoulos, Q. C. Zhong, and W. L. Ming, "PLL-Less Non-linear Current-Limiting Controller for Single-Phase Grid-Tied Inverters: Design, Stability Analysis, and Operation under Grid Faults," *IEEE Trans. Ind. Electron.*, vol. 63, no. 9, pp. 5582–5591, 2016.
- [20] L. Huang *et al.*, "A Virtual Synchronous Control for Voltage-Source Converters Utilizing Dynamics of DC-Link Capacitor to Realize Self-Synchronization," *IEEE J. Emerg. Sel. Top. Power Electron.*, vol. 5, no. 4, pp. 1565–1577, 2017.
- [21] H. K. Khalil, *Nonlinear Systems*. Englewood Cliffs, NJ, USA: Prentice-Hall, 2001.
- [22] Q.-C. Zhong and G. C. Konstantopoulos, "Current-Limiting Three-Phase Rectifiers," *IEEE Trans. Ind. Electron.*, vol. 65, no. 2, pp. 957–967, 2018.
- [23] R. Teodorescu, M. Liserre, and P. Rodriguez, *Grid Converters for Photovoltaic and Wind Power Systems*, Chichester, West Sussex, UK: Wiley, 2011.
- [24] Q. C. Zhong and Y. Zeng, "Universal Droop Control of Inverters with Different Types of Output Impedance," *IEEE Access*, vol. 4, pp. 702–712, 2016.
- [25] G. C. Konstantopoulos, Q. C. Zhong, B. Ren, and M. Krstic, "Bounded Integral Control of Input-to-State Practically Stable Nonlinear Systems to Guarantee Closed-Loop Stability," *IEEE Trans. Automat. Contr.*, vol. 61, no. 12, pp. 4196–4202, 2016.